

Topology Inference with Multivariate Cumulants: The Möbius Inference Algorithm

Kevin D. Smith, Saber Jafarpour, Ananthram Swami, and Francesco Bullo

Abstract—Many tasks regarding the monitoring, management, and design of communication networks rely on knowledge of the routing topology. However, the standard approach to topology mapping—namely, active probing with traceroutes—relies on cooperation from increasingly non-cooperative routers, leading to missing information. Network tomography, which uses end-to-end measurements of additive link metrics (like delays or log packet loss rates) across monitor paths, is a possible remedy. Network tomography does not require that routers cooperate with traceroute probes, and it has already been used to infer the structure of multicast trees. This paper goes a step further. We provide a tomographic method to infer the underlying routing topology of an arbitrary set of monitor paths, based on the joint distribution of end-to-end measurements. Our approach, called the *Möbius Inference Algorithm* (MIA), uses cumulants of this distribution to quantify high-order interactions among monitor paths, and it applies Möbius inversion to “disentangle” these interactions. We provide three variants of MIA. MIA-T precisely recovers the topology from exact cumulants. MIA-E uses hypothesis testing with a novel statistic, allowing for data-driven topology estimation. Finally, MIA-F provides a modification to MIA-T and MIA-E to significantly reduce the typical computational complexity, under an additional mild assumption. We present numerical examples for all three variants of MIA, including a case study based on the IEEE 118 test case.

Index Terms—Topology inference, network tomography, cumulants, high-order statistics.

I. INTRODUCTION

Many tasks regarding the monitoring, management, and design of communication networks benefit from the network operator’s ability to determine the routing topology, i.e., the incidence between paths and links in the network. During small-scale network failures, for example, routes may automatically switch, and it is important that the network operator have knowledge of the new routing matrix. In the case of large-scale topology failures, inference of the routing topology is a crucial prelude to determining both the surviving network topology and the available services that remain. Peer-to-peer file-sharing networks are another example: nodes may want to know the routing topology so that they can select routes that have minimal overlap with existing routes, so as to avoid congestion and improve performance. Additional applications to the inference of dark networks and adversarial networks is obvious. Furthermore, the problem of optimal monitor placement relies on some knowledge of the network topology, and inference of

the routing matrix provides topological information that could be used to bootstrap new end-to-end measurements.

Literature Review: Two main approaches are available for topology inference in communication networks: using *traceroutes*, and using *network tomography* [1]. Traceroutes are the simplest and most direct approach, but they rely on intermediate routers to cooperate by responding to traceroute packets. This cooperation is becoming increasingly uncommon [2], leading to inaccuracies in traceroute-based topology mapping [3]. Some authors modified traceroute approaches to account for uncooperative routers [4], [5], [6], using partial traceroute results to over-estimate the topology, then applying heuristics and side information to merge nodes. These approaches are intuitive and perform well on test cases, but a rigorous method of selection among viable topologies would still be desirable.

Another approach to topology inference has started to emerge from the literature on network tomography. Network tomography is the problem of inferring additive link metrics (like delays or log packet loss rates) from end-to-end measurements—a nice review is provided in [7]. Unlike traceroute approaches, network tomography does not rely on intermediate routers to cooperate with traces; instead, it measures the total delay, packet loss rate, etc. of packets sent across paths between hosts, and it solves a linear inverse problem to infer metrics on each link. While most tomography literature assumes that the topology is known, some authors have started using tomographic approaches to infer routing topology in special cases. The most common approach is to infer “path sharing metrics,” i.e., metrics for the segments that pairs of paths share in common, and to find a topology that can explain the path sharing metrics and the end-to-end measurements [8], [9]. This approach uniquely leads to the correct topology when applied to multicast trees [10], [11], [12], [13], [14], as well as to a class of directed acyclic networks [15]. More generally, [16] provides necessary and sufficient conditions for when network reconstruction is possible based on these “second-order” statistics (i.e., statistics involving pairs of monitor paths). Other approaches to network tomography have been developed to provide robustness against changing topologies [17], [18], but these techniques cannot be used for a wholesale reconstruction of the routing matrix. To our knowledge, no tomographic approaches are available to reconstruct general routing topologies from scratch.

Contributions: This paper provides such an approach. We extend the use of second-order path sharing metrics into higher-order statistics (i.e., statistics involving pairs of paths), allowing us to relax any underlying assumptions about the underlying topology. Our approach uses cumulants to

This work was supported in part by the U.S. Defense Threat Reduction Agency under grant HDTRA1-19-1-0017.

Kevin D. Smith, Saber Jafarpour, and Francesco Bullo are with the Center of Control, Dynamical Systems and Computation, UC Santa Barbara, CA 93106-5070, USA. {kevinsmith, saber, bullo}@ucsb.edu

Ananthram Swami is with the Army Research Laboratory.

quantify high-order interactions between sets of paths, then applies Möbius inversion to “disentangle” these interactions, resulting in an encoding of the routing topology. We envision several applications for our technique: improving the selection of topologies from partial traceroute information, identifying changes in topology, or even—as we consider in this paper—reconstructing topologies without any prior information.

Consider the usual setting for network tomography: there is a communication network consisting of nodes and links, in which packets accumulate some kind of metric as they traverse each link (e.g., a time delay or a log loss probability), and the sum of these metrics can be measured when packets are sent across certain monitor paths in the network. In the classical tomography setting, the experimenter knows which links are used by each monitor path; this incidence information is encoded in a known binary routing matrix. We provide a new technique for tomographic inference of the routing matrix. Our general approach, which we call the *Möbius Inference Algorithm* (MIA), is a non-parametric method of reconstructing the routing matrix from multivariate cumulants of end-to-end measurements, under mild assumptions. It does not require any prior knowledge of the topology or distributions of link metrics, and works under general routing topologies.

The paper has three main contributions. First, we provide a novel application of statistics and combinatorics to network tomography. We show that multivariate cumulants of end-to-end measurements reveal interactions between the monitor paths (in the form of overlapping links), and we demonstrate how Möbius inversion (on the Boolean lattice) can be used to infer link-path incidence from these cumulants. Based on these observations, we construct the *Theoretical Möbius Inference Algorithm* (MIA-T), which recovers a provably correct routing matrix from these cumulants.

Second, we provide a framework for routing matrix inference when a dataset of end-to-end measurements is available, instead of exact cumulants. This framework, called the *Empirical Möbius Inference Algorithm* (MIA-E), applies a hypothesis test to every candidate column of the routing matrix, deciding based on the data whether or not the column is present. This hypothesis testing is based on a novel statistic, and it works within any framework for location testing the mean of a distribution from a sample.

Third, we show how to significantly improve the performance of MIA-T and MIA-E under an additional assumption. The resulting algorithm, called the *Efficient Möbius Inference Algorithm* (MIA-F), uses a breadth-first-search procedure to substantially restrict the search space for columns of the routing matrix. It also minimizes the order of cumulants that must be evaluated (in the theoretical setting) or estimated (in the empirical setting).

We also provide several minor contributions. We offer a detailed examples that show how to apply MIA-T and MIA-E to a small test case, and we provide a numerical case study that shows the viability of MIA-F on a larger example, based on the IEEE 118 test case. Furthermore, through a numerical study of several random graph models, we investigate how the number and order of monitor path interactions scales with the number of monitor paths.

Organization: Section II begins to lay the groundwork for MIA. It formally describes the communication network model and key variables (II-A), reviews key definitions and notation (II-B), and discusses three assumptions that are invoked in various results throughout the paper (II-C).

The main theoretical content of the paper is presented in Section III. The section is organized around MIA-T (Algorithm 1) and its guarantees (Theorem 1), with the middle three subsections each describing one of the three stages of the algorithm. The section concludes with an walkthrough of MIA-T, applied to a small example (III-D).

Section IV adapts MIA to the case where data is available, instead of precise cumulants. The section begins with MIA-E (Algorithm 2), introduces our new test statistic (Definition 8), and discusses various hypothesis testing schemes that can exploit this statistic to determine if a candidate column of the routing matrix exists (IV-A). Again, the section concludes with an application of the algorithm to a small example (IV-B).

In Section V, we tackle the problem of computational efficiency. We first observe through numerical random graph experiments that interactions between monitor paths are typically sparse and of low order (V-A). Motivated by this observation, we construct MIA-F, which automatically exploits this sparsity to reduce the search space for routing matrix columns (V-B). We then show how to use MIA-F in place of either MIA-T or MIA-E (V-C).

Finally, Section VI applies MIA-F to a synthetic dataset based on the IEEE 118 test case.

II. MODELING AND PRELIMINARIES

A. Model

We consider a network on a (possibly directed) graph $G = (\mathcal{V}, \mathcal{L})$, where \mathcal{V} is a set of nodes, and $\mathcal{L} = \{\ell_1, \ell_2, \dots, \ell_m\}$ is a set of m links. Every link is associated with an additive link metric, like a time delay or log packet loss rate. For concreteness, we will refer to these metrics simply as “delays,” although other metrics are possible.

For each link, there is a *link delay variable* U_ℓ , which is a random variable representing the amount of time that a unit of traffic requires to traverse the link. Link delays are not measured directly. Instead, we will infer properties of these variables from cumulative delays across certain paths in G , called *monitor paths*. Let \mathcal{P} be a set of n monitor paths, which can be any simple paths in G . Each monitor path $p \in \mathcal{P}$ is associated with a *path delay variable*

$$V_p = \sum_{\substack{\ell \in \mathcal{L} \\ p \text{ traverses } \ell}} U_\ell, \quad \forall p \in \mathcal{P} \quad (1)$$

which is the total delay experienced by a unit of traffic along the path p . If we define a vector of link variables $U = (U_{\ell_1} \ U_{\ell_2} \ \dots \ U_{\ell_m})^\top$ and a vector of path variables $V = (V_{p_1} \ V_{p_2} \ \dots \ V_{p_n})^\top$, then we can write (1) in the form

$$V = RU \quad (2)$$

using a *routing matrix* $R \in \{0, 1\}^{n \times m}$, where $R_{p\ell} = 1$ if and only if p traverses the link ℓ .

We suppose that an experimenter is capable of measuring path delays $V_p(t)$ for each monitor path p , at many sample times $t = 1, 2, \dots, T$. The experimenter has no prior knowledge about the link variables U_ℓ , and—in contrast to most of the literature on network tomography—the experimenter does not know the routing matrix R . Importantly, we make the simplifying assumption in this paper that *link delays are spatially and temporally independent*, i.e., $U_\ell(t)$ and $U_{\ell'}(t')$ are statistically independent unless $\ell = \ell'$ and $t = t'$. This assumption is common in the network tomography literature.

B. Preliminaries and Notation

General Notation: Let $\mathbb{Z}_{\geq 0}$ and $\mathbb{Z}_{> 0}$ denote the sets of non-negative and positive integers, respectively. Given a set S and an integer $k \leq |S|$, let the binomial $\binom{S}{k} = \{S' \subseteq S : |S'| = k\}$ denote the collection of all k -element subsets of S . Given $k, n \in \mathbb{Z}_{\geq 0}$, let $\binom{n}{k}$ denote the number of k -element multisets chosen from n distinct elements. Given two ordered and countable sets $X \subseteq Y$, define the *characteristic vector* $\chi_Y(X) \in \{0, 1\}^{|Y|}$ of X in Y by $(\chi_Y(X))_i = 1$ if and only if $y_i \in X$.

Multi-Indices: A *multi-index* on a set S is any function $\alpha : S \rightarrow \mathbb{Z}_{\geq 0}$, which maps each element of S to a multiplicity. The *support* of a multi-index is the set of elements with positive multiplicity, i.e., $\text{supp}(\alpha) = \{s \in S : \alpha(s) \geq 1\}$. The *size* of a multi-index is its total multiplicity: $|\alpha| = \sum_{s \in S} \alpha(s)$. If S is an ordered set with n elements (e.g., if S consists of elements of a vector), then multi-indices on S are naturally represented as vectors $\alpha \in \mathbb{Z}_{\geq 0}^n$; in this case, we will use multi-indices on S and vectors in $\mathbb{Z}_{\geq 0}^n$ interchangeably.

Link Sets: Throughout this paper, we make use of two maps from sets of monitor paths to sets of links. Let $R \in \{0, 1\}^{n \times m}$ be the routing matrix. For each $P \in 2^{\mathcal{P}}$, we define the *common link set* $L_R : 2^{\mathcal{P}} \rightarrow 2^{\mathcal{L}}$ by

$$L_R(P) = \{\ell \in \mathcal{L} : p \in P \implies r_{p\ell} = 1\} \quad (3)$$

and the *exact link set* $M_R : 2^{\mathcal{P}} \rightarrow 2^{\mathcal{L}}$ by

$$M_R(P) = \{\ell \in \mathcal{L} : p \in P \iff r_{p\ell} = 1\} \quad (4)$$

The common link set $L_R(P)$ contains all links that are utilized by every path in P . The exact link set is more strict: $M_R(P)$ consists of links that are utilized by every path in P and that are not utilized by any path outside of P . Neither of these maps are known *a priori*. It is worth noting that the exact link set contains all of the information of the routing matrix, since $M_R(P)$ is nonempty if and only if the characteristic vector $\chi_{\mathcal{P}}(P)$ is a column of R .

Cumulants and k -Statistics: *Cumulants* are a class of statistical moments, which extend the familiar notions of mean and covariance to higher orders. A good introduction is provided in [19]. Minimum-variance unbiased estimates of cumulants are given by Fisher's *k-statistics*. The state-of-the-art treatment in [20] uses a formalism called the “umbral calculus” to derive k -statistics, and software packages are available to compute them, both in R [21] and Python [22].

Both cumulants and k -statistics come in two flavors: univariate (referencing a single random variable), and multivariate. In

this paper, univariate cumulants are always taken with respect to link delay variables. Given any link delay variable U_ℓ and any order $k \in \mathbb{Z}_{> 0}$, we use the notation $\kappa_k(U_\ell)$ to denote the k th-order univariate cumulant of the random variable U_ℓ . Furthermore, multivariate cumulants are always taken with respect to the joint distribution of path delays. Given any multi-index α on \mathcal{P} , we use the notation

$$\kappa_\alpha(V) = \kappa \left(\underbrace{V_{p_1}, \dots, V_{p_1}}_{\alpha_1 \text{ times}}, \dots, \underbrace{V_{p_n}, \dots, V_{p_n}}_{\alpha_n \text{ times}} \right)$$

to denote a $|\alpha|$ -order multivariate cumulant of the path delay variables. For example, given a multi-index $\alpha = (1, 2, 1)$ on the path set $\mathcal{P} = \{p_1, p_2, p_3\}$, we denote the corresponding fourth-order multivariate cumulant by $\kappa_{(1,2,1)}(V) = \kappa(V_1, V_2, V_2, V_3)$. We adopt similar notation for k -statistics, using $k_k(x_1, x_2, \dots, x_N)$ to represent the k th-order univariate k -statistic from a sample of points $x_t \in \mathbb{R}$, and using $k_\alpha(x_1, x_2, \dots, x_N)$ to denote the multivariate k -statistic of the data $x_t \in \mathbb{R}^n$ corresponding to a multi-index $\alpha \in \mathbb{Z}_{\geq 0}^n$.

C. Assumptions

At various points throughout the paper, we will invoke three closely-related assumptions regarding the routing matrix and link delay cumulants. Several of these assumptions have a “weak” version and a “strong” version. We will be explicit about which assumptions are required for any result that uses them. The first assumption requires that R has no repeated columns:

Assumption 1 (Distinct Links). No two links are traversed by precisely the same set of paths in \mathcal{P} ; i.e., no two columns of R are identical; i.e., $|M_R(P)| \in \{0, 1\}$ for all $P \in 2^{\mathcal{P}}$.

This assumption is common in the network tomography literature. If $\ell, \ell' \in \mathcal{L}$ are used by precisely the same set of monitor paths, then the link delays $U_\ell, U_{\ell'}$ will only show up in path delays through their sum $U_\ell + U_{\ell'}$. Due to this linear dependence, complete network tomography is impossible when Assumption 1 is violated, since R will be rank-deficient.

The second assumption requires that link delays have nonzero cumulants:

Assumption 2 (Nonzero Cumulants). For all $\ell \in \mathcal{L}$, and for $k = n$ (weak) or for all $k = 2, 3, \dots, n$ (strong), $\kappa_k(U_\ell) \neq 0$.

This assumption is necessary because MIA uses link delay cumulants as “tags” to detect that links are present. We consider this assumption to be realistic: zero-valued cumulants arise from symmetries within the distribution that have no reason to emerge in real-world link delays. For example, the normal distribution has zero-valued cumulants above order two, but link delays cannot possibly be normally distributed (as they are positive-valued). In fact, the normal distribution is the *only* distribution with a finite number of nonzero cumulants [19], so neither form of Assumption 2 is particularly restrictive.

Finally, the third assumption requires that certain *sums* of link delays have nonzero cumulants:

Assumption 3 (Nonzero Common Cumulants). For all $P \in 2^{\mathcal{P}}$, and for $k = n$ (weak) or for all $k = 2, 3, \dots, n$ (strong), if $L_R(P)$ is nonempty, then $\sum_{\ell \in L_R(P)} \kappa_k(U_\ell) \neq 0$.

In other words, if all paths in $P \in 2^{\mathcal{P}}$ share a collection of common links $L_R(P)$, the delay cumulants on these common links should not cancel out. This is a weak assumption, given that such a cancellation is exceedingly unlikely.

III. THEORETICAL MÖBIUS INFERENCE

We now proceed with our main theoretical contribution: a simple algorithm to infer the routing matrix from multivariate cumulants of path latencies. In this section, we assume that precise values for these cumulants are available. The main result is Algorithm 1, called the *Theoretical Möbius Inference Algorithm* (MIA-T), which provides exact inference of the routing matrix from these cumulants, at least under Assumptions 1 and 2 (weak).

The algorithm occurs in three stages:

- (i) *Estimation*. Estimate a vector of multivariate cumulants of path latencies. This vector contains information about the links that are common to any given collection of paths. (The label “estimation” is a misnomer in the context of MIA-T, wherein cumulants are known precisely, but it will make more sense when we consider the “data-driven” version of the algorithm.)
- (ii) *Inversion*. Apply a Möbius inversion transformation to this vector of estimates. The vector resulting from this transformation contains the routing matrix, under a simple encoding. The transformation is linear, so this step can be viewed as a matrix-vector multiplication.
- (iii) *Reconstruction*. Decode the transformed vector, thereby reconstructing the routing matrix.

Algorithm 1 Theoretical Möbius Inference Algorithm (MIA-T)

Input: Joint distribution of path delays $V = (V_{p_1} \ V_{p_2} \ \dots \ V_{p_n})^\top$

Output: Routing matrix \hat{R}

```

1: // Estimation stage:
2: Initialize undefined function  $f_n : 2^{\mathcal{P}} \rightarrow \mathbb{R}$ 
3: for  $P \in 2^{\mathcal{P}}$  :
4:   Define  $\alpha_P$  as any multi-index on  $\mathcal{P}$  such that
      $\text{supp}(\alpha) = P$  and  $|\alpha| = n$ 
5:    $f_n(P) \leftarrow \kappa_{\alpha_P}(V)$ 
6: // Inversion stage:
7: Initialize undefined function  $g_n : 2^{\mathcal{P}} \rightarrow \mathbb{R}$ 
8: for  $P \in 2^{\mathcal{P}}$  :
9:    $g_n(P) \leftarrow \sum_{Q \supseteq P} (-1)^{|Q|-|P|} f_n(Q)$ 
10: // Reconstruction stage:
11: Initialize empty matrix  $\hat{R} \in \mathbb{R}^{n \times 0}$ 
12: for  $P \in \text{supp}(g_n)$  :
13:    $\hat{R} \leftarrow (\hat{R} \ \chi_{\mathcal{P}}(P))$ 
14: return  $\hat{R}$ 
```

Theorem 1 (Analysis of MIA-T). Consider the application of Algorithm 1 to a joint distribution of path delays $V =$

$(V_{p_1} \ V_{p_2} \ \dots \ V_{p_n})^\top$. Let $R \in \{0, 1\}^{n \times m}$ be the true underlying routing matrix, and let $U = (U_{\ell_1} \ U_{\ell_2} \ \dots \ U_{\ell_m})^\top$ be the underlying link delays, so that $V = RU$. The following are true:

- (i) The algorithm terminates and returns a matrix $\hat{R} \in \{0, 1\}^{n \times \hat{m}}$ for some $\hat{m} \in \mathbb{Z}_{\geq 0}$, in $O(2^n)$ time.
- (ii) By line 6, the map $f_n : 2^{\mathcal{P}} \rightarrow \mathbb{R}$ satisfies the following property:

$$f_n(P) = \sum_{\ell \in L_R(P)} \kappa_n(U_\ell), \quad \forall P \in 2^{\mathcal{P}} \quad (5)$$

- (iii) By line 10, the map $g_n : 2^{\mathcal{P}} \rightarrow \mathbb{R}$ satisfies the following property:

$$g_n(P) = \sum_{\ell \in M_R(P)} \kappa_n(U_\ell), \quad \forall P \in 2^{\mathcal{P}} \quad (6)$$

- (iv) Every column of \hat{R} is also a column of R . Furthermore, if R and the underlying link distributions satisfy Assumptions 1 and 2 (weak), then R and \hat{R} are equivalent, up to a permutation of columns.

Statement (i) is obvious from inspection of the algorithm, so we will focus on proving the remaining three statements, which fall neatly into the three stages (estimation, inversion, and reconstruction) of the algorithm. In the following subsections, we will analyze each of these three stages.

A. Estimation Stage

The purpose of the estimation stage is to collect a vector of high-order statistics of path delays. These statistics are carefully chosen so that they contain information about the routing topology. The title of “estimation” for this stage will be more appropriate in the next subsection, when we must estimate these statistics from data (rather than compute them analytically from a known distribution).

In the estimation stage, we gather a vector of multivariate path delay cumulants for every path set $P \in 2^{\mathcal{P}}$. The multivariate cumulants that we select for each path set are based on representative multi-indices:

Definition 2 (Representative Multi-Indices). Let $P \in 2^{\mathcal{P}}$ be a path set, and let $k \geq |P|$ be an integer. A k th-order *representative multi-index* of P is any multi-index α on \mathcal{P} with the following two properties:

- (i) $\text{supp}(\alpha) = P$
- (ii) $|\alpha| = k$

We use the notation $\mathcal{A}_{k,P}$ to denote the set of all k th-order representative multi-indices of P .

We will now collect a vector of path delay cumulants, with one entry corresponding to each set of monitor paths in $2^{\mathcal{P}}$:

Definition 3 (Common Cumulant). Let k be a positive integer. For each $P \in 2^{\mathcal{P}}$, let α_P be any k th-order representative multi-index of P . The k th-order *common cumulant* is the vector $f_k : 2^{\mathcal{P}} \rightarrow \mathbb{R}$ with entries

$$f_k(P) = \kappa_{\alpha_P}(V), \quad \forall P \in 2^{\mathcal{P}} \quad (7)$$

Careful readers will also note that we refer to “the” common cumulant, rather than “a” common cumulant, which would seem more appropriate, given the many choices of representative multi-indices. But, as we will see, the value of the common cumulant is independent of the particular choice of representative multi-index. It turns out that the common cumulant for P , regardless of which representative multi-index we choose, is always the sum of univariate cumulants across links that are traversed by every path in P . Broadly speaking, the entries of f_k contain information about which links are common to every path in P .

Lemma 4 (Properties of the Estimation Stage). *The following are true:*

- (i) Let $P \in 2^{\mathcal{P}}$. If $k \geq |P|$, there are $\binom{k-1}{|P|-1}$ representative multi-indices of P .
- (ii) For all integers $k \geq 1$, the common cumulant $f_k : 2^{\mathcal{P}} \rightarrow \mathbb{R}$ satisfies (5).
- (iii) Statement (ii) of Theorem 1 is true, i.e., Algorithm 1 correctly computes the common cumulant vector for order $k = n$.

Proof. To prove (i), we will count the number of ways that k “counts” of multiplicity can be assigned to the support of a representative multi-index. Each element of P contains at least one count, and we are free to distributed the remaining $k - |P|$ counts arbitrarily across the elements of P . Thus, there are $\binom{|P|}{k - |P|}$ ways to distribute the remaining counts, which is equivalent to $\binom{k-1}{|P|-1}$.

To prove (ii), let α_P be some k th-order representative multi-index of P . Using the independence of U_ℓ and the multilinearity of multivariate cumulants, we have

$$\begin{aligned} f_k(P) &= \kappa \left(\underbrace{R^{(1)}U, \dots, R^{(1)}U}_{\alpha_P(1) \text{ times}}, \dots, \underbrace{R^{(n)}U, \dots, R^{(n)}U}_{\alpha_P(n) \text{ times}} \right) \\ &= \sum_{\ell=1}^m \left(r_{1\ell}^{\alpha_P(1)} \dots r_{n\ell}^{\alpha_P(n)} \right) \kappa \left(\underbrace{U_\ell, \dots, U_\ell}_{\alpha_P(1) + \dots + \alpha_P(n) \text{ times}} \right) \\ &= \sum_{\ell=1}^m \left(\prod_{i \in \text{supp}(\alpha_P)} r_{i\ell} \right) \kappa_k(U_\ell) \end{aligned}$$

where $R^{(i)}$ denotes the i th row of R . Since $\prod_{i \in \text{supp}(\alpha_P)} r_{i\ell} = 1$ if $\ell \in L_R(P)$ and is zero otherwise, we obtain (5).

To prove (iii), observe that the estimation stage of Algorithm 1 defines the map f_n precisely according to Definition 3, so that f_n is the common cumulant vector by line 6. Then (5) holds by statement (ii) of this lemma. \square

B. Inversion Stage

In the inversion stage, we extract topological information from the vector of common cumulants by applying an invertible linear transformation. Lemma 4 (ii) shows that common cumulants are sums over common link sets. But it is clear from (3) and (4) that common link sets can be written as unions of exact link sets, which more directly provide information about

the routing matrix. Accordingly, common cumulants can be written as sums over exact link sets, using *exact cumulants*:

Definition 5 (Exact Cumulant). Let $k \geq 1$ be an integer, and let R be a routing matrix. We define the k th-order *exact cumulant* $g_k : 2^{\mathcal{P}} \rightarrow \mathbb{R}$ by (6), with $n = k$.

In the following lemma, we formalize the relationship of common cumulants as sums of exact cumulants. We then apply Möbius inversion to this sum:

Lemma 6 (Properties of the Inversion Stage). *Let f_k be the common cumulant vector, and let $g_k : 2^{\mathcal{P}} \rightarrow \mathbb{R}$. The following three statements are equivalent:*

- (i) g_k is the exact cumulant vector.
- (ii) f_k and g_k satisfy

$$f_k(P) = \sum_{Q \supseteq P} g_k(Q), \quad \forall P \in 2^{\mathcal{P}} \quad (8)$$

- (iii) f_k and g_k satisfy

$$g_k(P) = \sum_{Q \supseteq P} (-1)^{|Q|-|P|} f_k(Q), \quad \forall P \in 2^{\mathcal{P}} \quad (9)$$

Furthermore, statement (iii) of Theorem 1 is true, i.e., the Algorithm 1 correctly computes the exact cumulant vector.

Proof. We begin with the equivalence (ii) \iff (iii). This equivalence holds for any functions $f_k, g_k : 2^{\mathcal{P}} \rightarrow \mathbb{R}$, and it follows from the Möbius inversion formula, applied over the poset of subsets of $2^{\mathcal{P}}$. See, for example, [23, Theorem 5.1].

To prove that (i) \implies (ii), we will first show that

$$L_R(P) = \bigcup_{Q \supseteq P} M_R(Q) \quad (10)$$

Let $\ell \in L_R(P)$, and examine the column of the routing matrix $R_\ell \in \{0, 1\}^n$. There is some $Q \in 2^{\mathcal{P}}$ for which the characteristic vector satisfies $\chi_{\mathcal{P}}(Q) = R_\ell$. It follows that $\ell \in M_R(Q)$. Now, because $\ell \in L_R(P)$, it follows that $r_{p\ell} = 1$ for all $p \in P$, so that $Q \supseteq P$. Therefore $\ell \in \bigcup_{Q \supseteq P} M_R(Q)$. Next, let $\ell \in \bigcup_{Q \supseteq P} M_R(Q)$, so that $\ell \in M_R(Q)$ for some $Q \supseteq P$. It is clear that $r_{p\ell} = 1$ for all $p \in Q$, so the inclusion $Q \supseteq P$ implies that $\ell \in L_R(P)$. Now, if g_k is the exact cumulant vector, we can substitute (10) into (6), obtaining

$$\begin{aligned} \sum_{Q \supseteq P} g_k(Q) &= \sum_{Q \supseteq P} \sum_{\ell \in M_R(Q)} \kappa_k(U_\ell) \\ &= \sum_{\ell \in L_R(P)} \kappa_k(U_\ell) \\ &= f_k(P) \end{aligned}$$

The last step follows from Lemma 4 (ii). Hence (i) \implies (ii).

To prove that (ii) \implies (i), suppose that f_k and g_k satisfy (8). By (10),

$$\sum_{Q \supseteq P} g_k(Q) = \sum_{Q \supseteq P} \sum_{\ell \in M_R(Q)} \kappa_k(U_\ell) \quad (11)$$

for all $P \in 2^{\mathcal{P}}$. We will use (11) to show that g_k satisfies (6), by strong induction over $|P|$. In the $|P| = n$ base case, the only possible set is $P = \mathcal{P}$, for which (11) reduces to $g_k(\mathcal{P}) = \sum_{\ell \in M_R(\mathcal{P})} \kappa_k(U_\ell)$. Now suppose that (6) holds for

all P with $|P| \leq i$ for some $i \in [2, n]$. Let $P \in 2^{\mathcal{P}}$ such that $|P| = i - 1$, and observe that

$$\sum_{Q \supseteq P} g_k(Q) = g_k(P) + \sum_{Q \supset P} \sum_{\ell \in M_R(Q)} \kappa_k(U_\ell)$$

by the inductive hypothesis. Substituting this equation in to (11) and simplifying, we obtain (6). Hence (6) holds for all $P \in 2^{\mathcal{P}}$, so (ii) \implies (i).

To prove the final statement, note that the inversion stage of Algorithm 1 defines the map g_n according to (9), where f_n is the common cumulant vector (per Lemma 4 (iii)), by line 10. It follows from the equivalence proven in this lemma that g_n is the exact cumulant vector. \square

Lemma 6 is the heart of MIA. By applying the inversion (9) to the vector of common cumulants, we calculate the vector of *exact* cumulants. Whereas common cumulants contain information about which links are traversed by every path in a set, exact cumulants contain information about which links are traversed *precisely* by the paths in a set, i.e., they contain information about columns of the routing matrix.

C. Reconstruction Stage

The final stage of the algorithm is to reconstruct the routing matrix from the exact cumulant vector. This reconstruction is straightforward, using only the zero-nonzero pattern of g_k :

Lemma 7 (Properties of the Reconstruction Stage). *Let $g_n : 2^{\mathcal{P}} \rightarrow \mathbb{R}$ be the exact cumulant vector. For each $P \in 2^{\mathcal{P}}$, let $\chi_{\mathcal{P}}(P) \in \{0, 1\}^n$ be the characteristic vector of P in \mathcal{P} . The following are true:*

- (i) *If $P \in \text{supp}(g_n)$, then $\chi_{\mathcal{P}}(P)$ must be a column of the routing matrix. Under Assumptions 1 and 2 (weak), the converse is also true.*
- (ii) *Statement (iv) of Theorem 1 is true.*

Proof. If $g_n(P) \neq 0$, it is clear from (6) that $M_R(P)$ is non-empty, which implies that some column of the routing matrix R_ℓ satisfies $\chi_{\mathcal{P}}(P) = R_\ell$. Now suppose that Assumptions 1 and 2 (weak) are true. By Assumption 1, the set $M_R(P)$ is either empty or contains a single element. By Assumption 2 (weak), if $M_R(P)$ contains a single element ℓ , it must satisfy $\kappa_n(U_\ell) \neq 0$. Therefore, if $g_n(P) = 0$, under these two assumptions, it follows that $M_R(P)$ is empty. Hence $\chi_{\mathcal{P}}(P)$ is not a column of the routing matrix.

Per Lemma 6, the vector g_n in Algorithm 1 is the exact cumulant vector by line 10, so we can apply the above result to g_n in the reconstruction stage of the algorithm, yielding statement (iv) of Theorem 1. \square

D. Detailed Example

In order to illustrate MIA-T, we will apply the algorithm to a small example, consisting of 3 monitor paths that utilize three links. We will walk through each of the three stages of the algorithm in detail.

Setup: Consider a network with three monitor paths $\mathcal{P} = \{p_1, p_2, p_3\}$ and three links $\mathcal{L} = \{\ell_1, \ell_2, \ell_3\}$, with a routing matrix

$$R = \begin{matrix} & \begin{matrix} \ell_1 & \ell_2 & \ell_3 \end{matrix} \\ \begin{matrix} p_1 \\ p_2 \\ p_3 \end{matrix} & \begin{pmatrix} 1 & 1 & 0 \\ 1 & 0 & 1 \\ 0 & 0 & 1 \end{pmatrix} \end{matrix} \quad (12)$$

Clearly this routing matrix satisfies Assumption 1. Each of the three link delay distributions is exponential, with probability density functions

$$f_{u_\ell}(x) = \lambda_\ell e^{-\lambda_\ell x}, \quad \forall \ell \in \mathcal{L}$$

where we pick intensities $\lambda_{\ell_1} = 1$, $\lambda_{\ell_2} = 1.5$, and $\lambda_{\ell_3} = 2$ (in units of per millisecond). All cumulants of exponential distributions are positive, so the latency variables satisfy Assumption 2. We then invoke (2) to obtain the joint distribution of path delays. The cumulant generating function for this path delay distribution can be written

$$K(t) = c - \log(t_1 + t_2 - \lambda_1) - \log(t_1 - \lambda_2) - \log(t_2 + t_3 - \lambda_3)$$

for a constant c , and the path cumulants are easily computed from mixed partial derivatives of this function. For example, to compute the cumulant $\kappa_{(1,2,0)}(V)$, we evaluate

$$\kappa_{(1,2,0)}(V) = \frac{\partial^3}{\partial t_1 \partial t_2^2} K(t_1, t_2, t_3) \Big|_{t=0_3} = 2$$

We assume that the theoretical distribution of path delays is known—in particular, the cumulants $\kappa_\alpha(V)$ are known exactly—and our objective is to use these cumulants to infer the routing matrix, via Algorithm 1.

1) *Estimation Stage:* There are seven non-empty path sets in $2^{\mathcal{P}}$. Sets with one path only have one 3rd-order representative multi-index; for example, the path set $P = \{p_1\}$ has a unique representative multi-index $\alpha = (3, 0, 0)$. Sets with two paths have 2 representative multi-indices; for example, $P = \{p_1, p_2\}$ has $\alpha = (2, 1, 0)$ and $\alpha' = (1, 2, 0)$. The three-element path set $P = \mathcal{P}$ has only the one representative multi-index $\alpha = (1, 1, 1)$.

For each of these seven paths, we will select one of the representative multi-indices arbitrarily and collect them into the common cumulant vector. For example:

$$f_3 = \begin{pmatrix} f_3(\{p_1\}) \\ f_3(\{p_2\}) \\ f_3(\{p_3\}) \\ f_3(\{p_1, p_2\}) \\ f_3(\{p_1, p_3\}) \\ f_3(\{p_2, p_3\}) \\ f_3(\mathcal{P}) \end{pmatrix} = \begin{pmatrix} \kappa_{(3,0,0)}(V) \\ \kappa_{(0,3,0)}(V) \\ \kappa_{(0,0,3)}(V) \\ \kappa_{(1,2,0)}(V) \\ \kappa_{(1,0,2)}(V) \\ \kappa_{(0,1,2)}(V) \\ \kappa_{(1,1,1)}(V) \end{pmatrix} = \begin{pmatrix} 70/27 \\ 9/4 \\ 1/4 \\ 2 \\ 0 \\ 1/4 \\ 0 \end{pmatrix}$$

It is worth taking a moment to note that f_3 agrees with the (5), i.e., we can decompose the vector into univariate cumulants of link delays:

$$f_3 = \begin{pmatrix} \kappa_{(3,0,0)}(V) \\ \kappa_{(0,3,0)}(V) \\ \kappa_{(0,0,3)}(V) \\ \kappa_{(1,2,0)}(V) \\ \kappa_{(1,0,2)}(V) \\ \kappa_{(0,1,2)}(V) \\ \kappa_{(1,1,1)}(V) \end{pmatrix} = \begin{pmatrix} \kappa_3(U_1) + \kappa_3(U_2) \\ \kappa_3(U_1) + \kappa_3(U_3) \\ \kappa_3(U_3) \\ \kappa_3(U_1) \\ 0 \\ \kappa_3(U_3) \\ 0 \end{pmatrix} = \begin{pmatrix} 70/27 \\ 9/4 \\ 1/4 \\ 2 \\ 0 \\ 1/4 \\ 0 \end{pmatrix}$$

Of course, performing this decomposition relies on our prior knowledge of R and the link delay distributions, which are unavailable to the experimenter.

2) *Inversion Stage*: In order to obtain the exact cumulant vector g_3 from the common cumulant vector f_3 , we apply the Möbius inversion transformation (9). Note that this transformation is linear, and it can be represented in the matrix form $g_3 = X f_3$, where the matrix X contains the coefficients $(-1)^{|Q|-|P|}$:

$$\begin{pmatrix} g_3(\{p_1\}) \\ g_3(\{p_2\}) \\ g_3(\{p_3\}) \\ g_3(\{p_1, p_2\}) \\ g_3(\{p_1, p_3\}) \\ g_3(\{p_2, p_3\}) \\ g_3(\mathcal{P}) \end{pmatrix} = \underbrace{\begin{pmatrix} 1 & 0 & 0 & -1 & -1 & 0 & 1 \\ 0 & 1 & 0 & -1 & 0 & -1 & 1 \\ 0 & 0 & 1 & 0 & -1 & -1 & 1 \\ 0 & 0 & 0 & 1 & 0 & 0 & -1 \\ 0 & 0 & 0 & 0 & 1 & 0 & -1 \\ 0 & 0 & 0 & 0 & 0 & 1 & -1 \\ 0 & 0 & 0 & 0 & 0 & 0 & 1 \end{pmatrix}}_X \begin{pmatrix} f_3(\{p_1\}) \\ f_3(\{p_2\}) \\ f_3(\{p_3\}) \\ f_3(\{p_1, p_2\}) \\ f_3(\{p_1, p_3\}) \\ f_3(\{p_2, p_3\}) \\ f_3(\mathcal{P}) \end{pmatrix}$$

Evaluating this transformation, we obtain the following expression for the exact cumulant vector:

$$g_3 = \begin{pmatrix} g_3(\{p_1\}) \\ g_3(\{p_2\}) \\ g_3(\{p_3\}) \\ g_3(\{p_1, p_2\}) \\ g_3(\{p_1, p_3\}) \\ g_3(\{p_2, p_3\}) \\ g_3(\mathcal{P}) \end{pmatrix} = \begin{pmatrix} 16/27 \\ 0 \\ 0 \\ 2 \\ 0 \\ 1/4 \\ 0 \end{pmatrix}$$

We can verify that these values for g_3 agree with both (6) and (8). For example, the routing matrix (12) implies that $M_R(\{p_1\}) = \{\ell_2\}$, so (6) gives

$$g_3(\{p_1\}) = \frac{2}{\lambda_{\ell_2}^3} = \frac{16}{27}$$

in agreement with our computed result for g_3 . Furthermore, (8) claims that we can decompose $f_3(\{p_1\})$ according to

$$\begin{aligned} f_3(\{p_1\}) &= g_3(\{p_1\}) + g_3(\{p_1, p_2\}) + g_3(\{p_1, p_3\}) + g_3(\mathcal{P}) \\ &= \frac{70}{27} \end{aligned}$$

in agreement with $f_3(\{p_1\})$ obtained from the previous stage.

3) *Reconstruction Stage*: All that remains is to examine the zero-nonzero pattern of g_3 . Note that g_3 has three non-zero entries: $P_1 = \{p_1\}$, $P_2 = \{p_1, p_2\}$, and $P_3 = \{p_2, p_3\}$. We can then reconstruct the routing matrix from the characteristic vectors of these three path sets:

$$\hat{R} = (\chi_{\mathcal{P}}(P_1) \quad \chi_{\mathcal{P}}(P_2) \quad \chi_{\mathcal{P}}(P_3)) = \begin{pmatrix} 1 & 1 & 0 \\ 0 & 1 & 1 \\ 0 & 0 & 1 \end{pmatrix}$$

Observe that \hat{R} is equivalent to the “ground truth” routing matrix in (12), modulo an irrelevant permutation of columns, as guaranteed by Theorem 1 (iv).

IV. EMPIRICAL MÖBIUS INFERENCE

Having presented the core theory underlying MIA, we now turn to a more practical problem: routing matrix inference from *data*, rather than from a theoretical distribution of path delays. Data requires us to use estimates of cumulants instead of exact values, which introduces noise into the inference procedure. Therefore, in order to develop an empirical inference procedure, we must account for noise in our estimate.

We begin by noting that Algorithm 1 could be considerably abbreviated—the only purpose of the estimation and inversion stages is to compute the exact cumulant vector, $g_n : 2^{\mathcal{P}} \rightarrow \mathbb{R}$. If we were willing to start with g_n as an input to the algorithm, all we would need to do is go through each entry of the vector, check if the entry is nonzero, and if so, append a certain column to the routing matrix. A similar approach applies to the empirical case; the only difference is that checking if $g_n(P) = 0$ relies on hypothesis testing.

Suppose that we have a hypothesis test $\text{IsNonzero}(g_n(P) \mid v_1, v_2, \dots, v_N)$, which decides whether or not to reject the null hypothesis that $g_n(P) = 0$, conditioning on a sample of path delays v_1, v_2, \dots, v_N . Given this test, *Empirical Möbius Inference Algorithm* (MIA-E) is succinctly stated:

Algorithm 2 Empirical Möbius Inference Algorithm (MIA-E)

Input: Path delay sample v_1, v_2, \dots, v_N , hypothesis test $\text{IsNonzero}(g_n(P) \mid v_1, v_2, \dots, v_N)$

Output: Routing matrix estimate \hat{R}

- 1: // *Reconstruction stage*:
 - 2: Initialize empty matrix $\hat{R} \in \mathbb{R}^{n \times 0}$
 - 3: **for** $P \in 2^{\mathcal{P}}$:
 - 4: **if** $\text{IsNonzero}(g_n(P) \mid v_1, v_2, \dots, v_N)$:
 - 5: $\hat{R} \leftarrow (\hat{R} \quad \chi_{\mathcal{P}}(P))$
 - 6: **return** \hat{R}
-

Clearly the performance of Algorithm 2 depends entirely on the accuracy of the hypothesis test. Of course, this accuracy depends on the test itself, the choice of test parameters (like significance levels), and the size of the sample size N , so it is difficult to state general theoretical guarantees regarding the algorithm. Nonetheless, some guarantees are evident in extreme cases, if Assumptions 1 and 2 (weak) are satisfied:

- (i) If the test has no Type I error, i.e., if $g_n(P) = 0$ always leads to a decision that $\text{IsNonzero}(g_n(P) \mid v_1, v_2, \dots, v_N)$ is false, then every column of \hat{R} will be a true column of R .
- (ii) If the test has no Type II error, then \hat{R} will contain every column of R .
- (iii) If the test is *consistent*, in the sense that the test is free of both Type I and Type II error in $N \rightarrow \infty$ limit, then similarly $\hat{R} = R$ in the $N \rightarrow \infty$ limit.

For all practical purposes, none of these extreme cases will apply, and we will have to rely on the algorithm’s performance in test scenarios to assess its usefulness.

A. Hypothesis Tests for the Exact Cumulant

We now describe several possible implementations of the $\text{IsNonzero}(g_n(P) \mid v_1, v_2, \dots, v_N)$ test. All of these implementations rely on the following statistic, which consolidates the estimation and inversion stages of the algorithm:

Definition 8 (Column Statistic). Let $k \geq 2$ be an integer. For each $P \in 2^{\mathcal{P}}$, we define a k th-order *column statistic* as a function $\hat{g}_{k,P} : \mathbb{R}^n \times \mathbb{R}^n \times \dots \times \mathbb{R}^n \rightarrow \mathbb{R}$ given by

$$\hat{g}_{k,P}(v_1, \dots, v_\ell) = \sum_{Q \supseteq P} (-1)^{|Q|-|P|} \sum_{\alpha \in \mathcal{A}_{k,P}} \lambda_\alpha k_\alpha(v_1, \dots, v_\ell) \quad (13)$$

where $\mathcal{A}_{k,P}$ is the set of k th-order representative multi-indices of P , the coefficients λ_α define any convex combination over $\mathcal{A}_{k,P}$, and $k_\alpha(\cdot)$ is the multivariate k -statistic for the multi-index α . Note that the column statistic is well-defined so long as the arity ℓ is at least k .

The inner sum of the column statistic is a convex combination of k -statistics, evaluated at different k th-order representative multi-indices of the same path set. Because k -statistics are unbiased estimators of cumulants, it follows from Definition 3 that the inner sum is an unbiased estimator of the common cumulant, $f_k(P)$. Then the outer sum applies the Möbius inversion from (9), resulting in an unbiased estimate of the exact cumulant, $g_k(P)$. (Relating the column statistic back to MIA-T: the inner sum encodes the estimation stage, and the outer sum applies the inversion stage.)

The column statistic enjoys the following properties:

Lemma 9 (Properties of the Column Statistic). *Let $2 \leq k \leq \ell$ be integers, and let V_1, V_2, \dots, V_ℓ be independent copies of the path delay distribution V . For each $P \in 2^{\mathcal{P}}$, the following are true:*

- (i) $\mathbb{E}[\hat{g}_{k,P}(V_1, V_2, \dots, V_\ell)] = g_k(P)$, i.e., $\hat{g}_{k,P}$ is an unbiased estimator for the exact cumulant.
- (ii) In the limit as $\ell \rightarrow \infty$, the distribution of $\sqrt{\ell}(\hat{g}_{k,P}(V_1, V_2, \dots, V_\ell) - g_k(P))$ converges in probability to a normal distribution with zero mean and constant variance.

Proof. We have already argued statement (i). Statement (ii) follows because k -statistics belong to a broader class of statistics known as U -statistics, and it is well-known that U -statistics obey the stated convergence in probability to a normal distribution (see, for example, [24]). \square

Because column statistics are an unbiased estimator of exact cumulants, we can assess the null hypothesis $g_n(P) = 0$ via an equivalent null hypothesis, that $\mathbb{E}[\hat{g}_{k,P}] = 0$ with order $k = n$. There is no single correct way to perform this test—many approaches exist, with advantages and disadvantages. We will list a few techniques here:

1) *Normal Approximation:* Because column statistics are asymptotically normally distributed, we could simply estimate the mean and variance of the distribution and apply a standard z -test. This approach is used in [25], for example, to perform hypothesis testing on univariate cumulants, using univariate k -statistics. Unfortunately, while the mean of the column statistic

distribution is easily estimated by $\hat{g}_{k,P}$, the variance relies on computing variances of multivariate k -statistics, which are both mathematically and computationally complex for orders larger than $k = 3$. Furthermore, the normal approximation may not become valid until the sample is very large.

2) *Sample Splitting:* Another simple approach is to partition the original N -length sample into M subsamples of size N/M , compute the column statistic for each subsample, and use standard hypothesis testing to assess whether the statistics have zero mean. Since the subsamples are non-overlapping, each of the M values of the column statistic will be iid, so standard approaches (like the 1-sample Student's t -test [26, §9.5]) can be used to test the null hypothesis that $\mathbb{E}[\hat{g}_{k,P}] = 0$. There is a tradeoff in choosing M . If M is too small, then then the t -test may behave poorly; but if M is too large, then the small size of each subsample will lead to wider variance in the column statistics.

3) *Jackknifing:* The jackknife [27] is a resampling technique wherein we remove one observation at a time from the sample. For $t = 1, 2, \dots, N$, let $\hat{g}_{k,P}^{(-t)} = \hat{g}_{k,P}(v_1, \dots, v_{t-1}, v_{t+1}, \dots, v_N)$ be the column statistic computed from all but the t th observation, and let $g_{k,P}^{(0)} = \hat{g}_{k,P}(v_1, \dots, v_N)$ be column statistic computed from the entire sample. For each t , we define a *pseudo-values* $g_{k,P}^{(t)} = N g_{k,P}^{(0)} - (N-1) \hat{g}_{k,P}^{(-t)}$. Classically, it is assumed that the pseudo-values are approximately independently distributed according to the distribution of $g_{k,P}^{(0)}$, so once again, a 1-sample Student's t -test (or a similar test) can be applied to the pseudo-values to assess the null hypothesis $\mathbb{E}[\hat{g}_{k,P}] = 0$.

4) *Bootstrapping:* Bootstrapping (see, e.g., [28, Chapter 2]) is a modern resampling technique that uses the empirical distribution (i.e., the discrete distribution with uniform weight on each sample value) to approximate the original distribution. For $b = 1, 2, \dots, M$ given some large M , we define a *resample* $\tilde{v}_{b1}, \tilde{v}_{b2}, \dots, \tilde{v}_{bN}$ that is chosen randomly with replacement from the original sample v_1, v_2, \dots, v_N . We then compute the column statistic for each resample, resulting in a sample of M column statistics, which we can use to perform a mean hypothesis test. This approach has been applied to estimating confidence intervals for cumulants [29].

B. Detailed Example

Setup: In order to illustrate the empirical version of the Möbius Inference Algorithm, we will continue to use the low-dimensional example from Section III-D, with the same routing matrix (12) and the same exponentially-distributed link delays. In order to create a synthetic dataset, we draw 900 independent samples from each link distribution. We obtain samples of V_{p_1} by summing the samples of U_{ℓ_1} and U_{ℓ_2} , and we similarly create 900 samples of V_{p_2} and V_{p_3} based on the sums encoded in the routing matrix.

Column Statistics: Before we apply hypothesis testing, we must define a suitable column statistic $\hat{g}_{3,P}$ for each of the seven non-empty path sets $P \in 2^{\mathcal{P}}$. Recall from Section III-D that path sets with size $|P| = 1$ or $|P| = 3$ have a unique 3rd-order representative multi-index (i.e., $|\mathcal{A}_{3,P}| = 1$), so there is only one possible column statistic for these path

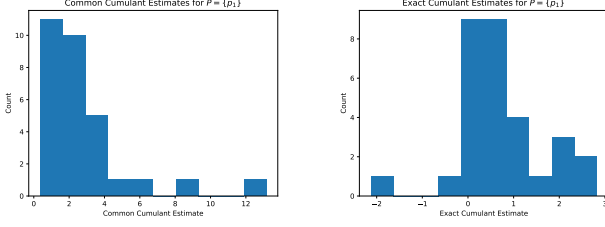


Fig. 1: Histogram of common cumulant estimates $\hat{f}_{3,\{p_1\}}$ (left) and column statistics $\hat{g}_{3,\{p_1\}}$ (right).

P	$f_3(P)$	$\hat{f}_{3,P}$	$g_3(P)$	$\hat{g}_{3,P}$
$\{p_1\}$	2.59	2.67 ± 0.5	0.593	0.66 ± 0.2
$\{p_2\}$	2.25	2.31 ± 0.7	0	0.06 ± 0.2
$\{p_3\}$	0.25	0.24 ± 0.05	0	0.02 ± 0.02
$\{p_1, p_2\}$	2	2.01 ± 0.6	2	2.01 ± 0.5
$\{p_1, p_3\}$	0	-0.01 ± 0.05	0	-0.01 ± 0.04
$\{p_2, p_3\}$	0.25	0.23 ± 0.07	0.25	0.23 ± 0.06
$\{p_1, p_2, p_3\}$	0	0.00 ± 0.09	0	0.00 ± 0.09

TABLE I: Coincident measures and inference measures in the low-dimensional example. Columns $f_3(P)$ and $g_3(P)$ report the true underlying values of the measure, while $\hat{f}_3(P)$ and $\hat{g}_3(P)$ show the mean and standard error of the respective estimates, $\hat{f}_3^s(P)$ and $\hat{g}_3^s(P)$.

sets. The remaining path sets have size $|P| = 2$, so there are two multi-indices in $\mathcal{A}_{3,P}$. It is unclear that we should favor one of these multi-indices over the other, so we choose the column statistic that simply uses their average.

It will be instructive to split the construction of the column statistics into two steps. In the first step, we define an intermediate statistic

$$\hat{f}_{k,P}(v_1, \dots, v_\ell) = \sum_{\alpha \in \mathcal{A}_{k,P}} \lambda_\alpha k_\alpha(v_1, \dots, v_\ell)$$

which we recognize as an unbiased estimator of the common cumulant $f_k(P)$. Based on the choices of representative multi-indices described above, we obtain a vector of statistics

$$\hat{f}_3(\cdot) = \begin{pmatrix} \hat{f}_{3,\{p_1\}}(\cdot) \\ \hat{f}_{3,\{p_2\}}(\cdot) \\ \hat{f}_{3,\{p_3\}}(\cdot) \\ \hat{f}_{3,\{p_1,p_2\}}(\cdot) \\ \hat{f}_{3,\{p_1,p_3\}}(\cdot) \\ \hat{f}_{3,\{p_2,p_3\}}(\cdot) \\ \hat{f}_{3,\mathcal{P}}(\cdot) \end{pmatrix} = \begin{pmatrix} k_{(3,0,0)}(\cdot) \\ k_{(0,3,0)}(\cdot) \\ k_{(0,0,3)}(\cdot) \\ \frac{1}{2}k_{(1,2,0)}(\cdot) + \frac{1}{2}k_{(2,1,0)}(\cdot) \\ \frac{1}{2}k_{(1,0,2)}(\cdot) + \frac{1}{2}k_{(2,0,1)}(\cdot) \\ \frac{1}{2}k_{(0,1,2)}(\cdot) + \frac{1}{2}k_{(0,2,1)}(\cdot) \\ k_{(1,1,1)}(\cdot) \end{pmatrix}$$

The vector of column statistics is obtained by $\hat{g}_3(\cdot) = X \hat{f}_3(\cdot)$, where X is the matrix defined in Section III-D.

Hypothesis Testing: We will use the sample splitting approach to the $\text{IsNonzero}(g_k(P) \mid v_1, v_2, \dots, v_N)$ test in this example. The 900 original sample points are split into 30 samples of size 30, and independent column statistics are computed from each of the 30 samples. Figure 1 visualizes the distribution of these statistics for a single path set, $P = \{p_1\}$. The left histogram plots the distribution of cumulant estimates $\hat{f}_{3,\{p_1\}}$, and the right histogram shows the distribution of column statistics $\hat{g}_{3,\{p_1\}}$. While the empirical $\hat{f}_{3,\{p_1\}}$ distribution is quite skewed, the sample mean of 2.67 is close

P	p-value for $g_3(P) = 0$	$\chi(P)$ is in R ?
$\{p_1\}$	0.001	Yes
$\{p_2\}$	0.8	No
$\{p_3\}$	0.5	No
$\{p_1, p_2\}$	0.0005	Yes
$\{p_1, p_3\}$	0.9	No
$\{p_2, p_3\}$	0.0008	Yes
$\{p_1, p_2, p_3\}$	1	No

TABLE II: Hypothesis testing for whether or not $\chi(P)$ is a column of the routing matrix, at 0.01 significance.

to the true common cumulant $f_3(\{p_1\}) = 70/27$ computed in Section III-D. Similarly, the sample mean of the column statistic distribution is 0.59, close to the exact cumulant value $g_3(\{p_1\}) = 16/27$. Table I reports the sample means and standard errors for the empirical $\hat{f}_{3,P}$ and column statistic distributions for all path sets. Indeed, *all* of the $\hat{f}_{3,P}$ and $\hat{g}_{3,P}$ sample means are within one standard error of $f_3(P)$ and $g_3(P)$, respectively.

We use a 1-sample Student's t -test to assess the null hypothesis that $E[\hat{g}_{3,P}] = g_3(P) = 0$ for each path set. The p -value for each null hypothesis is reported in Table II, as well as the result of the test with a significance threshold of 0.01.

Reconstruction Stage: Using the last column of Table II, which reports the result of the $\text{IsNonzero}(g_k(P) \mid v_1, v_2, \dots, v_N)$ hypothesis test for each path set, we can very quickly “run” Algorithm 2. For precisely three of the path sets, we reject the null hypothesis that $g_3(P) = 0$: $P_1 = \{p_1\}$, $P_2 = \{p_1, p_2\}$, and $P_3 = \{p_2, p_3\}$. Assembling the characteristic vectors of these path sets into \hat{R} , we obtain

$$\hat{R} = (\chi_{\mathcal{P}}(P_1) \quad \chi_{\mathcal{P}}(P_2) \quad \chi_{\mathcal{P}}(P_3)) = \begin{pmatrix} 1 & 1 & 0 \\ 0 & 1 & 1 \\ 0 & 0 & 1 \end{pmatrix}$$

which is identical to our result from Section III-D, and is identical to the ground truth routing matrix (up to a permutation of columns).

V. COMPLEXITY REDUCTION

In the previous two sections, we demonstrated two algorithms to infer the routing matrix from path latencies: one from theoretical distributions (MIA-T), and one from data (MIA-E). Unfortunately, both algorithms run in $O(2^n)$ time, rendering them impractical for systems with many more than 20 monitor paths. More concerning, MIA-E relies on k -statistics of order n , while both the computation and variance of k -statistics scale poorly with increasing order. It is necessary to reduce both the number and order of k -statistics, in order to apply MIA to anything beyond small-scale scenarios.

This section addresses both of these problems. In V-A, we observe that the common cumulant vector is typically very sparse, and that usually only the smallest path sets have a common link. We use these observations in V-B to design a routing inference procedure that is more efficient, but still exact. The resulting algorithm, called the *Efficient Möbius Inference Algorithm* (MIA-F), still has worst-case $O(2^n)$ complexity, but it is much faster in most realistic scenarios, and it relies on k -statistics of smaller order.

Graph	Model	Nodes	Edges
BA 2	Barabási-Albert ($k = 2$)	100	197
BA 5	Barabási-Albert ($k = 5$)	100	485
WS 2	Watts-Strogatz ($k = 2, p = 0.01$)	100	200
WS 5	Watts-Strogatz ($k = 5, p = 0.01$)	100	500
ER 200	Erdős-Renyi	100	200
ER 500	Erdős-Renyi	100	500

TABLE III: Specifications of the random graph models used to assess sparsity metrics. For Barabási-Albert graphs, k is the number of edges added each step. For Watts-Strogatz graphs, k is the regularity of the initial graph, and p is the re-wiring probability.

A. Sparsity of the Common Cumulant Vector

In many cases, the vector of common cumulants is sparse. For any order k , recall that $f_k(P)$ is nonzero only if every path in P shares a common link, i.e., only if $L_R(P)$ is non-empty. It is easy to see that L_R has the monotonicity property that $L_R(Q) \subseteq L_R(P)$ for all $Q \supseteq P$. Therefore, if $L_R(P)$ is empty, it follows not only that $f_k(P) = 0$, but also that $f_k(Q) = 0$ for all larger path sets $Q \supseteq P$. In other words, given that $L_R(P) = \emptyset$ for a single path set P , we can immediately infer that $2^{|P|}$ entries of the common cumulant vector are zero-valued. It seems that f_k ought to be sparse, and that the non-zero entries of f_k ought to favor small path sets.

In this subsection, we will examine how the underlying routing matrix R affects the coincident measure sparsity. We first define two closely related metrics for the sparsity of f_k , both of which are based entirely on the routing matrix. The *counting density* ρ_{count} quantifies the number of path sets in 2^P that share a common link:

$$\rho_{\text{count}}(R) = |\{P \in 2^P : |L_R(P)| \geq 1\}|$$

Since $f_k(P) = 0$ if P does not admit a common link, the routing matrix bounds the number of non-zero entries in f_k by $|\text{supp}(f_k)| \leq \rho_{\text{count}}(R)$. Second, the *max order density* ρ_{max} identifies the size of the largest path set with a common link:

$$\rho_{\text{max}}(R) = \max_{P \in 2^P} \{|P| : |L_R(P)| \geq 1\}$$

The max order density bounds the size of P for non-zero entries in f_k , since $|P| \leq \rho_{\text{max}}(R)$ for all $P \in \text{supp}(f_k)$. Of course, these two values are related; it is easy to verify that

$$2^{\rho_{\text{max}}(R)} \leq \rho_{\text{count}}(R) \leq \sum_{j=1}^{\rho_{\text{max}}(R)} \binom{n}{j}$$

It can also be shown that the right-most quantity in this inequality is order $O(2^{\rho_{\text{max}}(R)})$.

We will use several random graph models to study how ρ_{count} and ρ_{max} scale with the number of monitor paths, n . We consider 6 random models for an underlying 100-node graph: two Barabási-Albert models, two Watts-Strogatz models, and two Erdős-Renyi models, where one of each is tuned to approximately 200 edges, and the other tuned to 500 edges. (See Table III for detailed model specifications.) For each model, we generate 100 sample routing matrices with the following procedure:

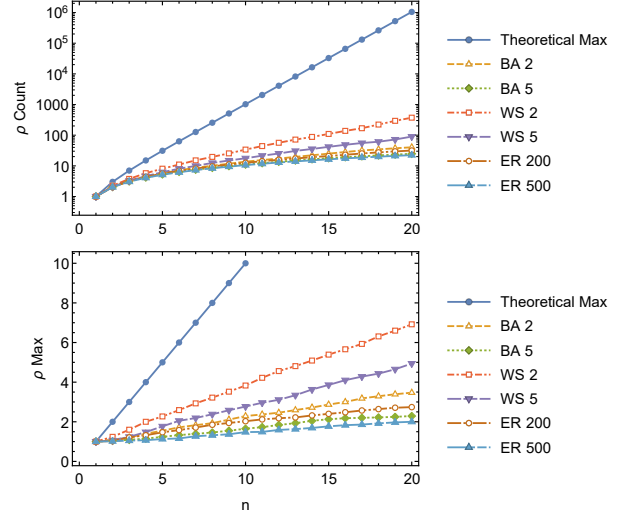


Fig. 2: Sparsity metrics in sparsity in random graphs. The top plot shows ρ_{count} on a log scale, and the bottom plot shows ρ_{max} on a linear scale.

- (i) Initialize a random graph with the given model, and select n source-target node pairs at random (without replacement).
- (ii) Find an unweighted shortest path for each source-target pair. Encode each of these n shortest paths into a routing matrix.

We then average $\rho_{\text{count}}(R)$ and $\rho_{\text{max}}(R)$ over each of the 100 routing matrices. Repeating this procedure for several different values of n , we obtain the plots in Figure 2. These plots reveal a pattern in all of the random graph models: $\rho_{\text{count}}(R)$ grows exponentially in n , and ρ_{max} grows linearly with n , with growth rates / slopes depending on the particular graph model. For all of the models, the growth rates of $\rho_{\text{count}}(R)$ and slopes of ρ_{max} are significantly smaller than those of the theoretical upper bounds.

In light of these results for random graphs, it would be reasonable for us to expect that $f_k(P) = 0$ for the vast majority of path sets $P \in 2^P$, and that $f_k(P) = 0$ for all path sets where $|P|$ exceeds some small fraction of n .

B. Efficient Möbius Inference Algorithm

We have made an argument that f_k ought to be sparse in most cases, and that the non-zero entries of f_k ought to correspond to small path sets. We will now design an inference procedure, called the *Efficient Möbius Inference Algorithm* (MIA-F), that is capable of exploiting these sparsity properties. Note that the sparsity of f_k is a motivation for MIA-F, and not a requirement—the algorithm still works with dense common cumulants vectors, but it automatically exploits any sparsity that is present, in order to reduce the number and order of k -statistic evaluations.

Unlike MIA-T and MIA-E, which loop through all 2^n entries of f_k , MIA-F uses a breadth-first-search procedure to enumerate $\text{supp}(f_k)$. Central to this enumeration is a structure called the *support graph*:

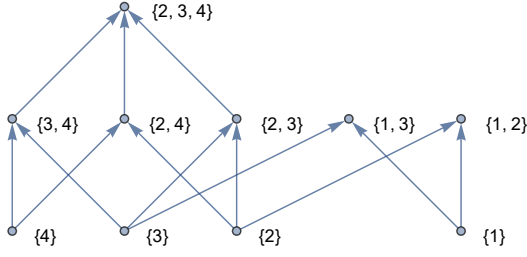


Fig. 3: Support graph for f_k in Example 11. Nodes are labeled with path set indices; e.g., the node $\{3, 4\}$ corresponds to the path set $\{p_3, p_4\}$.

Definition 10 (Support Graph). Let $f_k : 2^{\mathcal{P}} \rightarrow \mathbb{R}$ be a common cumulant vector for some order $k \in \{2, 3, \dots, n\}$. The *support graph* of f_k is the directed acyclic graph $G_f = (\mathcal{V}_f, \mathcal{E}_f)$, where $\mathcal{V}_f = \text{supp}(f_k)$, and $(P, Q) \in \mathcal{V}_f^2$ is an edge if and only if $Q = P \cup \{p\}$ for some $p \in \mathcal{P}$.

Example 11 (Support Graph). Consider a network with 4 monitor paths and 3 links, with the following routing matrix:

$$R = \begin{matrix} & \ell_1 & \ell_2 & \ell_3 \\ \begin{matrix} p_1 \\ p_2 \\ p_3 \\ p_4 \end{matrix} & \begin{pmatrix} 1 & 0 & 1 \\ 1 & 1 & 0 \\ 0 & 1 & 1 \\ 0 & 1 & 0 \end{pmatrix} \end{matrix}$$

Out of the 15 nonempty sets in $2^{\mathcal{P}}$, there are 10 sets that have a common link. Under Assumption 3 (strong), all of these sets have a non-zero common cumulant, for all orders $k = 2, 3, \dots, n$. Hence, precisely these 10 sets comprise $\text{supp}(f_k)$ for each order, and the support graphs G_f are identical for each order. Figure 3 depicts G_f .

The following lemma provides some basic properties of support graphs, which hints at why they are useful and how they might be computed. The first statement shows that what we observed in Example 11 is generally true: under Assumption 3 (strong), the support graph does not depend on the cumulant order. The second statement claims that all nodes in G_f are descendants of some singleton path set, which will allow us to construct G_f using breadth-first-search. Finally, the third statement shows we can identify and compute non-zero entries of g_k using only nodes of G_f .

Lemma 12 (Properties of the Support Graph). Let $f_k, g_k : 2^{\mathcal{P}} \rightarrow \mathbb{R}$ be common cumulant and exact cumulant vectors of each order $k = 2, 3, \dots, n$. Under Assumption 3 (strong), the following are true:

- (i) The support graphs corresponding to f_k for each $k = 2, 3, \dots, n$ are identical.
- (ii) Let G_f be the unique support graph from the previous statement. Then every singleton path set $P \in \binom{\mathcal{P}}{1}$ is a source node in G_f . Furthermore, if $P \in \text{supp}(f_k)$ with $|P| \geq 2$, then G_f contains a directed path from $\{p\}$ to P for all $p \in P$.
- (iii) For any $k = 2, 3, \dots, n$ and for all $P \in 2^{\mathcal{P}}$, precisely one of the following is true:

- a) P is not a node of G_f , and $g_k(P) = 0$.
- b) P is a node of G_f , and

$$g_k(P) = \sum_{Q \in \mathcal{D}(P)} (-1)^{|Q|-|P|} f_k(Q) \quad (14)$$

where $\mathcal{D}(\cdot)$ denotes the set of ancestors in G_f .

Proof. We first note that, under Assumption 3 (strong), the following equivalence holds for all $k = 2, 3, \dots, n$: $|L_R(P)| \geq 1$ if and only if $f_k(P) = 0$. This implies that $\text{supp}(f_k)$ are identical for all orders k , leading to (i). To prove (ii), let $P \in 2^{\mathcal{P}}$. If $|P| = 1$, then $L_R(P)$ is non-empty, so $P \in \text{supp}(f_k)$. Otherwise, if $P \in \text{supp}(f_k)$, then $L_R(P)$ is non-empty, which implies that $L_R(P')$ is non-empty for all subsets $P' \subseteq P$, which further implies that all subsets of P are nodes in G_f . Then the statement is clear by inspection of the edges between these subsets provided by Definition 10.

To prove (iii), let $P \in 2^{\mathcal{P}}$. It is clear from (9) that

$$g_k(P) = \sum_{Q \supseteq P: Q \in \text{supp}(f_k)} (-1)^{|Q|-|P|} f_k(Q)$$

If P is not a node of G_f , then $f_k(P) = 0$ and $f_k(Q) = 0$ for all $Q \supseteq P$, so there are no summands, and we obtain $g_k(P) = 0$. But if P is a node of G_f , we can see that $Q \supseteq P$ belongs to $\text{supp}(f_k)$ if and only if Q is a descendant of P , and we obtain (14). \square

We now state MIA-F. For brevity, and for generality (so that we do not need to state two different versions of the algorithm for theoretical and empirical settings), MIA-F does not include the computation of f_k or g_k (i.e., the estimation and inversion stages). Rather, the inputs to the algorithm are two “oracles” $\text{IsNonzero}(f_k(P))$ and $\text{IsNonzero}(g_k(P))$, which determine if $f_k(P) = 0$ or $g_k(P) = 0$, for any order $k = 2, 3, \dots, n$. These oracles depend on whether we are operating in the theoretical or empirical setting, and we will revisit them in detail in V-C. Regardless of the setting, MIA-F proceeds according to Algorithm 3.

The first for loop in the algorithm constructs the support graph of f_k . The graph G_f is initialized to contain every singleton path set. Thereafter, the i th iteration of the loop identifies all path sets of size i in $\text{supp}(f_i)$ and adds them to the graph (along with the appropriate edges). Note that the algorithm uses the smallest possible cumulant order to check whether each path set belongs to the support graph, exploiting the order-independence of the support graph under Assumption 3 (strong). The last for loop is simply the reconstruction stage—but instead of checking all 2^n possible path sets, the search is restricted to nodes in the support graph, which can significantly reduce the number of iterations. Again, we use the smallest order possible to check the exact cumulant.

Depending on the accuracy of the oracles, we can prove the following guarantees regarding MIA-F:

Theorem 13 (Analysis of MIA-F). Consider the application of Algorithm 3 to a pair of oracles $\text{IsNonzero}(f_k(P))$ and $\text{IsNonzero}(g_k(P))$. Let $f_k, g_k : 2^{\mathcal{P}} \rightarrow \mathbb{R}$ be the true common cumulant and exact cumulant vectors, and let R be

Algorithm 3 Efficient Möbius Inference Algorithm (MIA-F)

Input: Oracles $\text{IsNonzero}(f_k(P))$ and $\text{IsNonzero}(g_k(P))$, for orders $k = 2, 3, \dots, n$

Output: \hat{R} , an estimate of the routing matrix

- 1: Initialize empty matrix $\hat{R} \in \{0, 1\}^{n \times 0}$, initialize a graph $G_f = (\mathcal{V}_f, \mathcal{E}_f)$ with $\mathcal{V}_f = \binom{P}{1}$ and $\mathcal{E}_f = \emptyset$, initialize $\mathcal{L} = \binom{P}{1}$ and $\mathcal{L}' = \emptyset$
- 2: // Construct the support graph:
- 3: **for** $i = 2, 3, \dots, n$:
- 4: **for** $\{P_1, P_2, \dots, P_i\} \in \binom{\mathcal{L}}{i}$:
- 5: $Q \leftarrow P_1 \cup P_2 \cup \dots \cup P_i$
- 6: **if** $|Q| = i$ and $\text{IsNonzero}(f_i(Q))$:
- 7: Append Q to \mathcal{V}_f and \mathcal{L}'
- 8: **for** $j = 1, 2, \dots, i$:
- 9: Append (P_j, Q) to \mathcal{E}_f
- 10: $\mathcal{L} \leftarrow \mathcal{L}'$ and $\mathcal{L}' \leftarrow \emptyset$
- 11: // Reconstruction stage:
- 12: **for** $P \in \mathcal{V}_f$:
- 13: $k \leftarrow \max\{|Q| : Q \text{ is descendant of } P\}$
- 14: **if** $\text{IsNonzero}(g_k(Q))$:
- 15: Append $\chi(Q)$ as a column to \hat{R}
- 16: **return** \hat{R}

the true underlying routing matrix. Under Assumptions 1, 2 (strong), and 3 (strong), the following are true:

- (i) The algorithm terminates and returns a matrix $\hat{R} \in \{0, 1\}^{n \times \hat{m}}$ for some $\hat{m} \in \mathbb{Z}_{\geq 0}$.
- (ii) Let $\hat{G}_f = (\hat{\mathcal{V}}_f, \hat{\mathcal{E}}_f)$ be the final value of the variable $G_f = (\mathcal{V}_f, \mathcal{E}_f)$. We have the following guarantees:
 - a) If $\text{IsNonzero}(f_k(P))$ has no Type I error, i.e., if $\text{IsNonzero}(f_k(P))$ is true only if $P \in \text{supp}(f_k)$, then $\hat{\mathcal{V}}_f \subseteq \text{supp}(f_k)$.
 - b) If $\text{IsNonzero}(f_k(P))$ has no Type II error, i.e., if $\text{IsNonzero}(f_k(P))$ is false only if $f_k(P) = 0$, then $\hat{\mathcal{V}}_f \supseteq \text{supp}(f_k)$.
 - c) If $\text{IsNonzero}(f_k(P))$ has no Type I or Type II error, then \hat{G}_f is the support graph of f_k .
- (iii) If $\text{IsNonzero}(f_k(P))$ has no Type II error, we have the following guarantees:
 - a) If $\text{IsNonzero}(g_k(P))$ has no Type I error, then every column of \hat{R} is also a column of R .
 - b) If $\text{IsNonzero}(g_k(P))$ has no Type II error, then every column of R is also a column of \hat{R} .
 - c) If $\text{IsNonzero}(g_k(P))$ has no Type I or Type II error, then $\hat{R} = R$.
- (iv) Let s be the number of $\text{IsNonzero}(f_k(P))$ evaluations, let r be the number of $\text{IsNonzero}(g_k(P))$ evaluations, and let k^* be the largest order at which either oracle is evaluated. Then $r \leq s$, and if $\text{IsNonzero}(f_k(P))$ has no Type I error, $s \leq \rho_{\text{count}}(R) + \binom{n}{k^*}$ and $k^* \leq \rho_{\text{max}}(R) + 1$.

This theorem follows from simple but somewhat tedious bookkeeping, so we omit the proof in the interest of brevity.

Statements (ii) and (iii) provide basic guarantees regarding the algorithm's construction of the support graph and

routing matrix, respectively. Because the search for path sets in $\text{supp}(g_k)$ is restricted to nodes of the support graph, \hat{R} is only accurate if the support graph isn't missing any nodes. *Extra* nodes are less of a problem—provided that $\text{IsNonzero}(g_k(P))$ is sufficiently protective against Type I error, the only consequence of Type I error for $\text{IsNonzero}(f_k(P))$ is extra computation time, as unnecessary path sets are checked in the reconstruction stage. Therefore, Type I error is generally preferable to Type II error in $\text{IsNonzero}(f_k(P))$.

Statement (iv) demonstrates the improved efficiency of MIA-F. Recall that MIA-T and MIA-E compute all 2^n entries of f_k and g_k , and they use a cumulant order $k = n$. But MIA-F, provided that $\text{IsNonzero}(f_k(P))$ has a sufficiently low rate of Type I error, can be much more efficient. First, the algorithm does not evaluate cumulants in excess of $\rho_{\text{max}}(R) + 1$, which is typically considerably smaller than n . Second, the number of cumulant evaluations exceeds $\rho_{\text{max}}(R)$ by at most $\binom{n}{k^*}$ evaluations, usually leading to significantly fewer evaluations than 2^n . Of course, the worst-case performance of the algorithm still results in 2^n evaluations of n th-order cumulants—but, in most cases, we can expect a substantial improvement in runtime over the previous algorithms.

C. Oracles

The performance of MIA-F depends largely on the two oracles, $\text{IsNonzero}(f_k(P))$ and $\text{IsNonzero}(g_k(P))$. We will examine how these oracles are implemented in both the theoretical and empirical settings.

In the theoretical setting, i.e., when exact values of path delay cumulants are available, we can compute $f_k(P)$ and $g_k(P)$ directly. As in the estimation stage of MIA-T, we calculate $f_k(P)$ from multivariate cumulants of path delays using (7), and $\text{IsNonzero}(f_k(P))$ simply compares this value with zero. The $\text{IsNonzero}(g_k(P))$ oracle can use the support graph to simplify the calculation of $g_k(P)$ using (14), and compare this result with zero. Of course, both of these oracles have complete accuracy—there is no Type I or Type II error when exact values of path delay cumulants are known.

In the empirical setting, when cumulants must be estimated from data, the oracles represent hypothesis tests. Recall that the statistic

$$\hat{f}_{k,P}(v_1, \dots, v_\ell) = \sum_{\alpha \in \mathcal{A}_{k,P}} \lambda_\alpha k_\alpha(v_1, \dots, v_\ell) \quad (15)$$

where $\mathcal{A}_{k,P}$ is the set of k -th order representative multi-indices of P , and λ_α encode any convex combination, is an unbiased estimator of $f_k(P)$. The $\text{IsNonzero}(f_k(P))$ oracle can employ this statistic within any one of the testing paradigms discussed in IV-A, to assess the null hypothesis that $f_k(P) = \mathbb{E}[\hat{f}_{k,P}] = 0$.

The empirical $\text{IsNonzero}(g_k(P))$ oracle is precisely the $\text{IsNonzero}(g_k(P) \mid v_1, v_2, \dots, v_T)$ hypothesis test discussed in Section IV, so this oracle can use column statistics to assess the null hypothesis that $g_k(P) = \mathbb{E}[\hat{g}_{k,P}] = 0$. But, in light of Lemma 12 (iii), the oracle can use the support graph

to simplify this computation. Given an estimate of the support graph that isn't missing any nodes, the statistic

$$\tilde{g}_{k,P}(v_1, \dots, v_\ell) = \sum_{Q \in \mathcal{D}(P)} (-1)^{|Q|-|P|} \hat{f}_{k,P}(v_1, \dots, v_\ell) \quad (16)$$

which restricts the sum to descendants of P in the support graph, is an unbiased estimator of $g_k(P)$. Therefore, the $\text{IsNonzero}(g_k(P))$ can use $\tilde{g}_{k,P}$ as a more-efficient alternative to the column statistic.

VI. SYNTHETIC CASE STUDY

a) *Synthetic Dataset:* We chose the topology of the IEEE-118 test case for the underlying graph G . This graph consists of $|\mathcal{V}| = 118$ nodes and $m = 179$ links. Each link ℓ is assigned a gamma distribution $\Gamma(k_\ell, \theta)$ for the link delay, where we chose a uniform scale parameter $\theta = 4$, and we assigned shape parameters k_ℓ to ensure a desired average delay θk_ℓ . Average delays were chosen based on line resistances in the IEEE-118 test case. Given a line resistance r_ℓ , we specified average delays $\theta k_\ell = 1 + \max\{0, \log r_\ell\}$, in order to flatten the wide distribution of line resistances and impose a minimum latency on each link.

Out of the 118 nodes, we selected 5 monitor nodes and $\binom{5}{2} = 10$ monitor paths, according to the following criteria. First, the set of monitor paths is precisely the set of paths between each pair of monitor nodes. Second, the path between two nodes is assumed to be the shortest path, weighted by average link delay. Third, monitor nodes were chosen so that the corresponding monitor paths minimize overlap (so as to reduce the order of cumulants needed) and maximize coverage of edges. The selected monitor nodes correspond to a routing matrix $R \in \{0, 1\}^{10 \times 179}$, but the monitor paths only utilize 36 of the 179 links in G , and roughly half of the non-zero columns in R are duplicates. After removing the zero-valued and redundant columns (to satisfy Assumption 1), we are left with a routing matrix $R \in \{0, 1\}^{10 \times 17}$.

In order to create a synthetic dataset of path delays, we drew a sample of 100,000 joint delays for the 10 monitor paths. (This may correspond to, for example, one observation per second over 28 hours.)

b) *Methods:* We employed MIA-F to reconstruct the underlying routing matrix. Both the $\text{IsNonzero}(f_k(P))$ and $\text{IsNonzero}(g_k(P))$ hypothesis tests were implemented using sample splitting: the 100,000 observations were split into 100 sub-samples of length 1,000, and we used a 1-sample Student's t -test with the statistics (15) and (16) to assess the null hypotheses $f_k(P) = 0$ and $g_k(P) = 0$, respectively. We used a uniform significance threshold of 0.05.

All steps of the case study were implemented in Python, using the *PyMoments* library to compute multivariate k -statistics [22].

c) *Results and Discussion:* The support graph is shown in Figure 4. The estimated support graph (i.e., the value of \hat{G}_f immediately before Line 13) was exactly correct—nodes in the reconstructed support graph were in one-to-one correspondence with $P \in 2^{\mathcal{V}}$ with non-empty common link sets $L_R(P)$. This correctness of the support graph indicates

that our $\text{IsNonzero}(f_k(P))$ test did not yield any Type I or Type II error.

Figure 5 depicts how the reconstructed routing matrix \hat{R} (i.e., the output from Algorithm 3) compares to the ground truth. Of the $2^{10} - 1$ possible links, we identified 15 true positives and 1004 true negatives, with 2 false positives and 2 false negatives. Viewing the reconstruction procedure as a classifier of link existence, we had a classification accuracy of 0.996, and an F1 score of 0.882.

This experiment demonstrates the viability of MIA-F in a larger and somewhat more realistic test case than the small examples in III-D and IV-B. The ability to reconstruct an error-free support graph is especially promising, given that key performance guarantees in Theorem 13 depend on an accurate support graph.

VII. CONCLUSION

In this paper, we have used high-order statistics of the joint distribution of path delays, in order to uniquely recover the underlying routing matrix. The possibilities for extensions of this work are rich. An immediate problem of interest would be to incorporate side information, like using partial information from traceroutes (as in [30]), or including prior knowledge of the topology. Another relevant problem is how the routing topology relates to the physical network topology—i.e., how an estimate of the routing matrix constrains the underlying graph. The assumption of spatially and temporally independent link distributions should also be investigated, in order to make Möbius Inference Algorithm (and other tomography-based approaches) applicable to real-world datasets—perhaps by averaging or filtering procedures, or corrections for global correlations.

REFERENCES

- [1] X. Zhang and C. Phillips, "A survey on selective routing topology inference through active probing," *IEEE Communications Surveys & Tutorials*, vol. 14, no. 4, pp. 1129–1141, 2011.
- [2] M. H. Gunes and K. Sarac, "Analyzing router responsiveness to active measurement probes," in *International Conference on Passive and Active Network Measurement*, 2009, pp. 23–32.
- [3] M. Luckie, Y. Hyun, and B. Huffaker, "Traceroute probe method and forward ip path inference," in *ACM SIGCOMM Conference on Internet Measurement*, 2008, pp. 311–324.
- [4] B. Yao, R. Viswanathan, F. Chang, and D. Waddington, "Topology inference in the presence of anonymous routers," in *IEEE Conf. on Computer Communications*, vol. 1, 2003, pp. 353–363.
- [5] X. Jin, W.-P. K. Yiu, S.-H. G. Chan, and Y. Wang, "Network topology inference based on end-to-end measurements," *IEEE Journal on Selected Areas in Communications*, vol. 24, no. 12, pp. 2182–2195, 2006.
- [6] B. Holbert, S. Tati, S. Silvestri, T. La Porta, and A. Swami, "Network topology inference with partial information," *IEEE Transactions on Network and Service Management*, vol. 12, no. 3, pp. 406 – 419, 2015.
- [7] M. Coates, A. O. Hero III, R. Nowak, and B. Yu, "Internet tomography," *IEEE Signal Processing Magazine*, vol. 19, no. 3, pp. 47–65, 2002.
- [8] A. Anandkumar, A. Hassidim, and J. Kelner, "Topology discovery of sparse random graphs with few participants," *Random Structures & Algorithms*, vol. 43, no. 1, pp. 16–48, 2013.
- [9] A. Sabnis, R. K. Sitaraman, and D. Towsley, "OCCAM: An optimization based approach to network inference," *ACM SIGMETRICS Performance Evaluation Review*, vol. 46, no. 2, pp. 36–38, 2019.
- [10] S. Ratnasamy and S. McCanne, "Inference of multicast routing trees and bottleneck bandwidths using end-to-end measurements," in *IEEE Conf. on Computer Communications*, 1999, pp. 353–360.

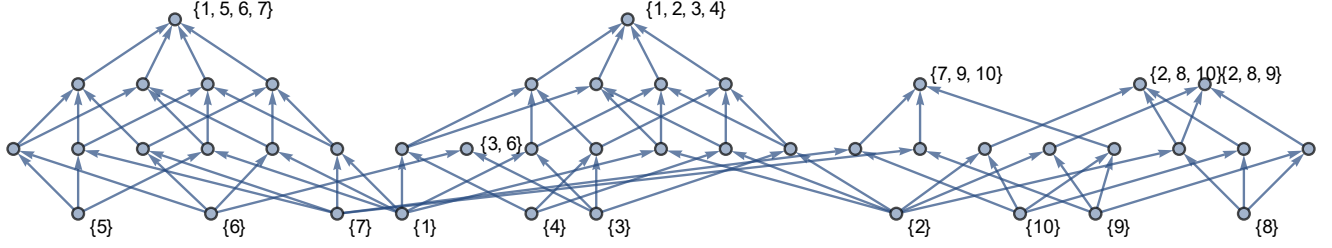


Fig. 4: Support graph for the IEEE-118 synthetic case study. Each node corresponds to a path set in $\text{supp}(f_k)$. Single-element path sets are in the first row, two-element path sets in the second row, and so on.

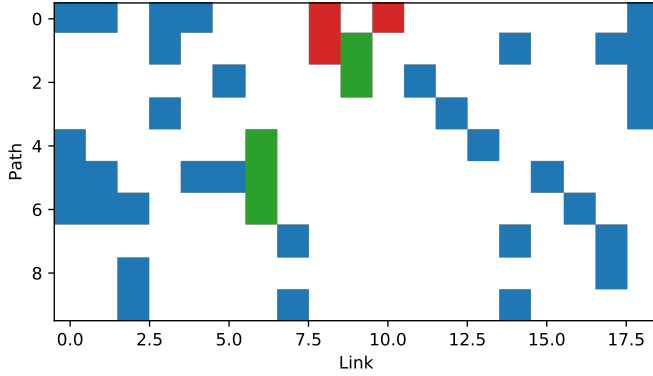


Fig. 5: Accuracy of the reconstructed routing matrix from the IEEE-118 case study. Rows correspond to paths, and columns correspond to links. Blue columns were correctly identified in the reconstructed matrix, red columns were missed by the inference (false negative), and green columns were erroneously included in the reconstructed matrix (false positive).

[11] N. G. Duffield, J. Horowitz, F. Lo Presti, and D. Towsley, "Multicast topology inference from measured end-to-end loss," *IEEE Transactions on Information Theory*, vol. 48, no. 1, pp. 26–45, 2002.

[12] M. Coates, R. Castro, R. Nowak, M. Gadhiok, R. King, and Y. Tsang, "Maximum likelihood network topology identification from edge-based unicast measurements," in *ACM SIGMETRICS Performance Evaluation Review*, 2002, pp. 11–20.

[13] A. Bestavros, J. W. Byers, and K. A. Harfoush, "Inference and labeling of metric-induced network topologies," *IEEE Transactions on Parallel and Distributed Systems*, vol. 16, no. 11, pp. 1053–1065, 2005.

[14] J. Ni, H. Xie, S. Tatikonda, and Y. R. Yang, "Efficient and dynamic routing topology inference from end-to-end measurements," *IEEE/ACM Transactions on Networking*, vol. 18, no. 1, pp. 123–135, 2009.

[15] P. Sattari, C. Fragouli, and Markopoulou, "Active topology inference using network coding," *Physical Communication*, vol. 6, pp. 142–163, 2013.

[16] G. Berkolaiko, N. Duffield, M. Ettehad, and K. Manousakis, "Graph reconstruction from path correlation data," *Inverse Problems*, vol. 35, no. 1, p. 015001, 2018.

[17] L. Ma, T. He, A. Swami, D. Towsley, and K. K. Leung, "Network capability in localizing node failures via end-to-end path measurements," *IEEE/ACM Transactions on Networking*, vol. 25, no. 1, pp. 434–450, 2016.

[18] A. Gkelias, L. Ma, K. K. Leung, A. Swami, and D. Towsley, "Robust and efficient monitor placement for network tomography in dynamic networks," *IEEE/ACM Transactions on Networking*, vol. 25, no. 3, pp. 1732–1745, 2017.

[19] P. McCullagh and J. Kolassa, "Cumulants," *Scholarpedia*, vol. 4, no. 3, p. 4699, 2009.

[20] E. D. Nardo, G. Guarino, and D. Senato, "A new method for fast computing unbiased estimators of cumulants," *Statistics and Computing*,

vol. 19, no. 2, p. 155, 2009.

[21] E. D. Nardo and G. Guarino, "kstatistics: Unbiased estimators for cumulant products," 2019, R package version 1.0. [Online]. Available: <https://CRAN.R-project.org/package=kStatistics>

[22] K. D. Smith, "PyMoments: A Python toolkit for unbiased estimation of multivariate statistical moments," 2020. [Online]. Available: <https://github.com/KevinDalySmith/PyMoments>

[23] M. Aigner, *A Course in Enumeration*. Springer, 2007.

[24] R. N. Sproule, "Asymptotic properties of U-statistics," *Transactions of the American Mathematical Society*, vol. 199, pp. 55–64, 1974.

[25] B. Staude, S. Rotter, and S. Grün, "CuBIC: cumulant based inference of higher-order correlations in massively parallel spike trains," *Journal of Computational Neuroscience*, vol. 29, no. 1-2, pp. 327–350, 2010.

[26] M. H. DeGroot and M. J. Schervish, *Probability and Statistics*, 4th ed. Pearson Education, 2012.

[27] R. G. Miller, "The jackknife-a review," *Biometrika*, vol. 61, no. 1, pp. 1–15, 1974.

[28] A. C. Davison and D. V. Hinkley, *Bootstrap Methods and Their Application*. Cambridge University Press, 1999.

[29] Y. Zhang, D. Hatzinakos, and A. N. Venetsanopoulos, "Bootstrapping techniques in the estimation of higher-order cumulants from short data records," in *IEEE Int. Conf. on Acoustics, Speech and Signal Processing*, vol. 4, 1993, pp. 200–203.

[30] B. Eriksson, P. Barford, and R. Nowak, "Network discovery from passive measurements," in *ACM SIGCOMM 2008 Conference on Data communication*, 2008, pp. 291–302.